**Stem Cell Reports, Volume *2***

# Supplemental Information

# Quality Metrics

# for Stem Cell-Derived Cardiac Myocytes

Sean P. Sheehy, Francesco Pasqualini, Anna Grosberg, Sung Jin Park, Yvonne Aratyn-Schaus, and Kevin Kit Parker

## Supplementary Figures

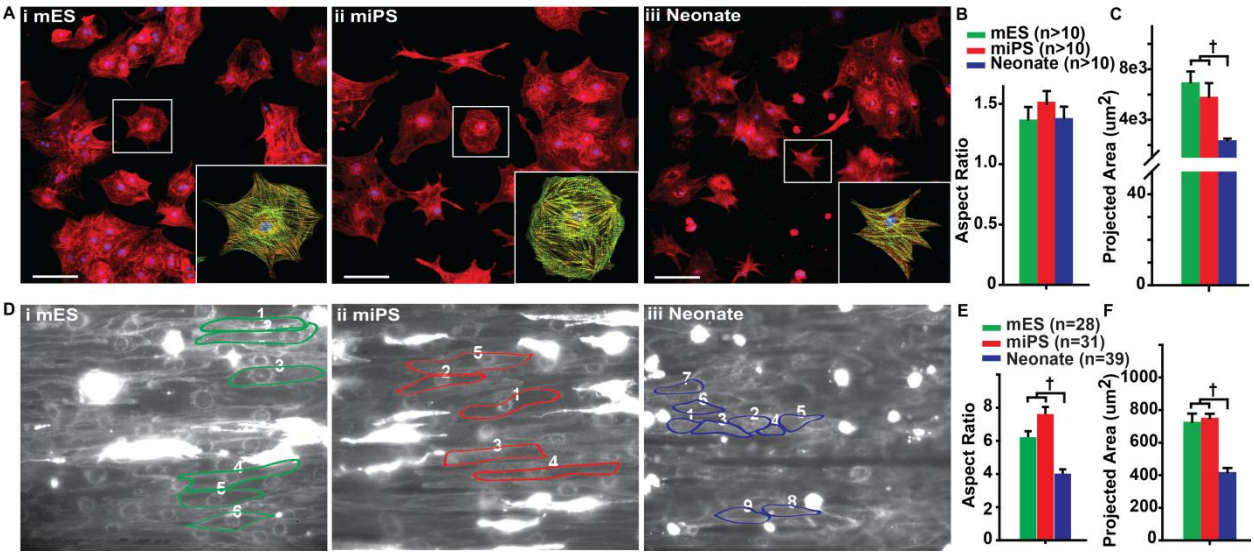


**Figure S1. Evaluation of myocyte morphology, related to Figure 1.** (**A**) Isotropic cultures of (**i**) mES, (**ii**) miPS, and (**iii**) neonate cardiac myocytes were fixed and immunostained for the presence of sarcomeric α-actinin (red), F-actin (green), and chromatin (blue). Cardiac myocytes were identified by the presence of sarcomeric α-actinin positive z-lines, and the boundaries of fully spread, mono-nucleated myocytes were manually traced using the polygon tool in ImageJ. The total number of pixels contained within each traced polygon was used to calculate (**B**) cellular aspect ratio, and (**C**) the total spread surface area for each cell type. (**D**) Similarly, the voltage sensitive dye RH237 used for optical mapping experiments allowed identification of myocyte boundaries in anisotropic monolayers of (**i**) mES, (**ii**) miPS, and (**iii**) neonate cardiac myocytes. The total number of pixels contained in each manually traced outline was used to calculate (**E**) aspect ratio, and (**F**) total spread surface area for each type of myocyte. All results presented as mean ± standard error of the mean. Statistical tests used was ANOVA on ranks († = $p < 0.05$). Scale bars = 20 μm.

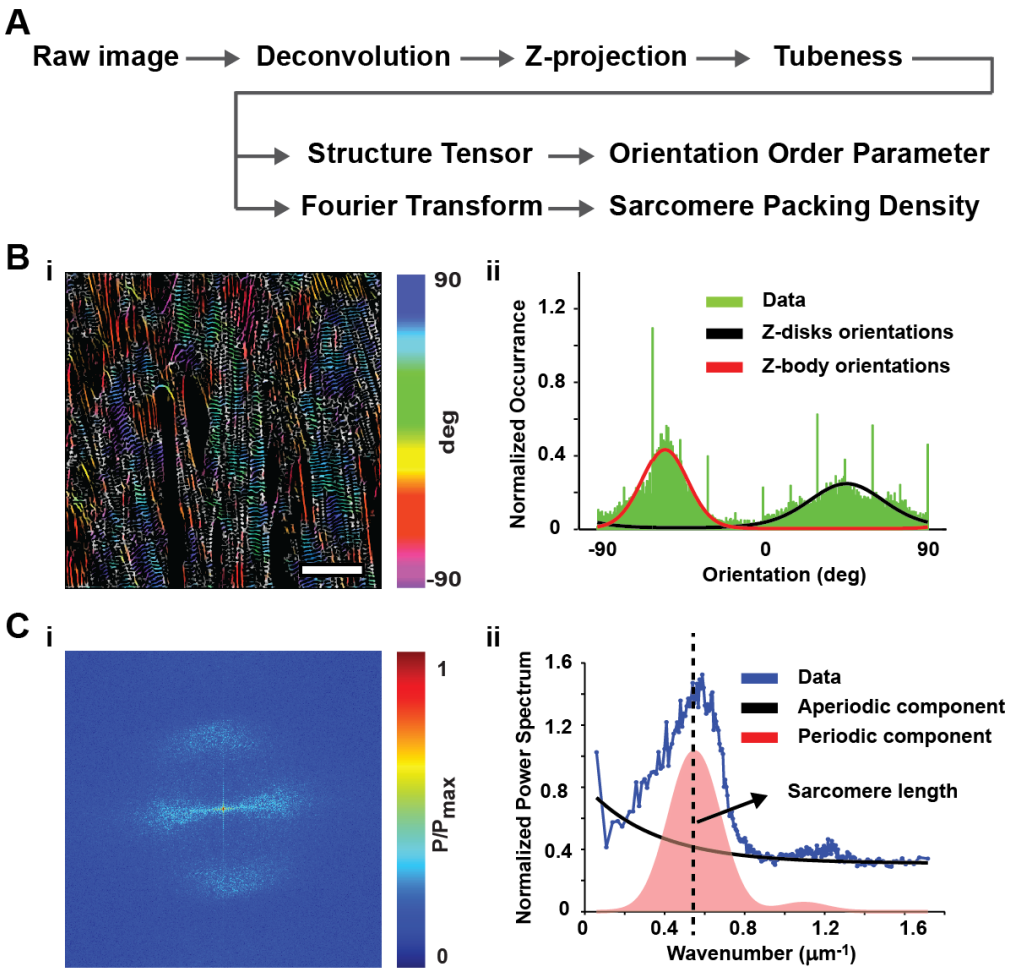


**Figure S2. Sarcomere structural characterization, related to Figure 2.** (**A**) Image processing flow: sarcomeric a-actinin immunographs were deconvolved, projected onto a single 2D image and then processed with a tubeness operator before further processing. (**B**) The orientations of sarcomeric a-actinin positive pixels were detected with a structure tensor method, color coded using the HSV digital image representation (**i**) and finally displayed into a histogram (**ii**) of the normalized occurrences of each orientation (**C**) The sarcomere length and the overall regularity of the cytoskeletal structure were detected processing the immunograph 2D Fast Fourier Transform algorithm. The detected power spectrum (**i**), for representation purpose a gamma correction of 0.1 was applied) was then integrated and normalized by the total energy. (**ii**) The sarcomere packing density was defined as the area under the signal peaks (red curve) whose location related with the sarcomere length.

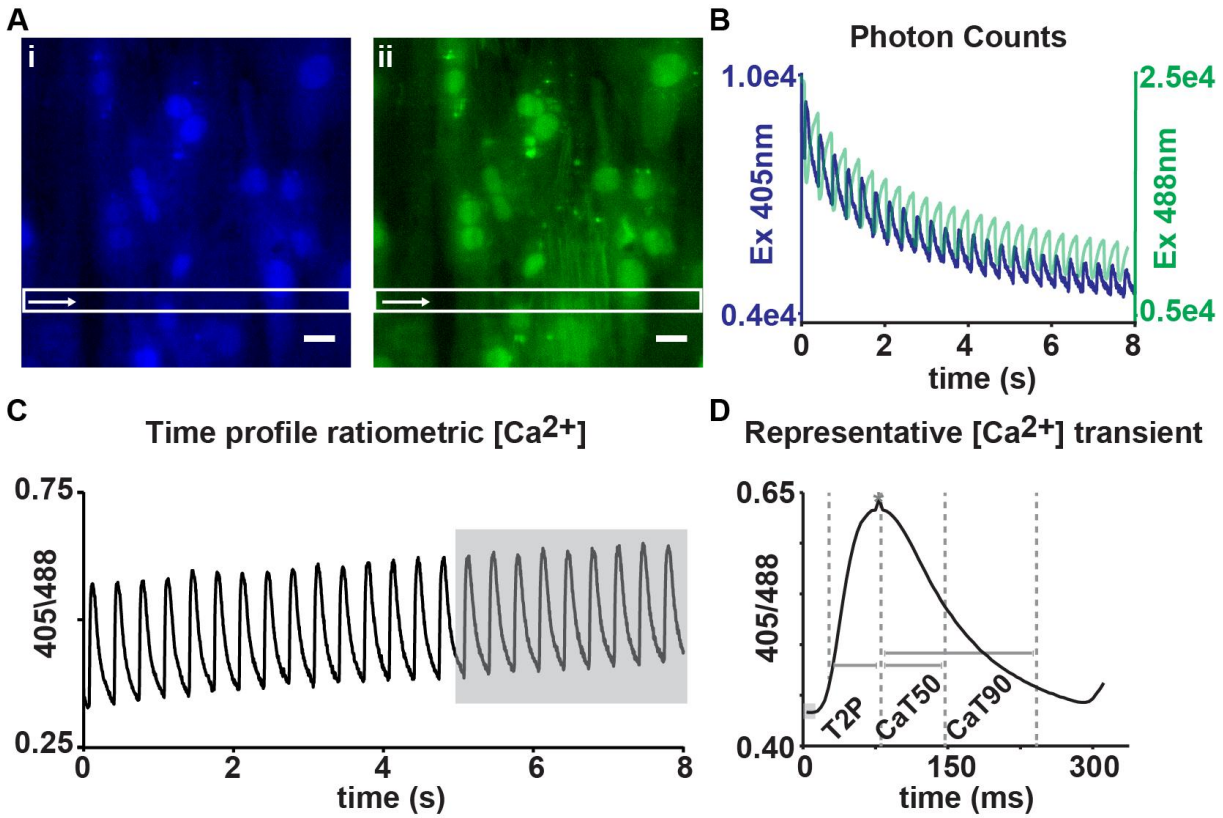


**Figure S3. Ratiometric $Ca^{2+}$ transient measurements, related to Figure 3.** (**A**) Anisotropic tissues were loaded with Fura-red and 20 lines (white box, direction indicated by the white arrow) were scanned in dual-excitation mode at 405 nm (**i**) and 488 nm (**ii**); the sampling frequency was 250 Hz. Scale bars = 15 μm. (**B**) The background-subtracted averaged number of photons collected with excitation at 405 nm (blue) and 488 nm (green) in each frame was used to obtain 2 signals proportional to the elevation of the cytoplasmic calcium in the tissue. (**C**) The ratio of these signals is an improved measurement of the calcium transient as bleaching and other artifacts are automatically corrected for. To further improve signal quality, 4-6 steady-state transients (grey box) were averaged (**D**) and the following quantities were calculated: diastolic level (grey box), peak level (*), time to peak (T2P) and the duration of the calcium transient at 50% (CaT50) and 90% (CaT90) decay.

## Supplementary Tables

### Table S1. Custom RT-qPCR array gene list, related to Figure 1

| Gene Symbol | Refseq # | Gene Description |
|---|---|---|
| *Hey2* | NM_013904 | Hairy/enhancer-of-split related with YRPW motif 2 |
| *Irx4* | NM_018885 | Iroquois related homeobox 4 (Drosophila) |
| *Bmp10* | NM_009756 | Bone morphogenetic protein 10 |
| *Gata4* | NM_008092 | GATA binding protein 4 |
| *Myocd* | NM_145136 | Myocardin |
| *Nkx2-5* | NM_008700 | NK2 transcription factor related, locus 5 (Drosophila) |
| *Tbx5* | NM_011537 | T-box 5 |
| *Nppa* | NM_008725 | Natriuretic peptide type A |
| *Acta1* | NM_009606 | Actin, alpha 1, skeletal muscle |
| *Adra1b* | NM_007416 | Adrenergic receptor, alpha 1b |
| *Adra2a* | NM_007417 | Adrenergic receptor, alpha 2a |
| *Actc1* | NM_009608 | Actin, alpha, cardiac muscle 1 |
| *Actn1* | NM_134156 | Actinin, alpha 1 |
| *Actn2* | NM_033268 | Actinin alpha 2 |
| *Pln* | NM_023129 | Phospholamban |
| *Tnnt2* | NM_011619 | Troponin T2, cardiac |
| *Ttn* | NM_011652 | Titin |
| *Myh6* | NM_010856 | Myosin, heavy polypeptide 6, cardiac muscle, alpha |
| *Myh7* | NM_080728 | Myosin, heavy polypeptide 7, cardiac muscle, beta |
| *Myl2* | NM_010861 | Myosin, light polypeptide 2, regulatory, cardiac, slow |
| *Myl3* | NM_010859 | Myosin, light polypeptide 3 |
| *Myl4* | NM_010858 | Myosin, light polypeptide 4 |
| *Myl7* | NM_022879 | Myosin, light polypeptide 7, regulatory |
| *Cacna1c* | NM_009781 | Calcium channel, voltage-dependent, L type, alpha 1C subunit |
| *Cacna1d* | NM_028981 | Calcium channel, voltage-dependent, L type, alpha 1D subunit |
| *Cacna1g* | NM_009783 | Calcium channel, voltage-dependent, T type, alpha 1G subunit |
| *Cacna1h* | NM_021415 | Calcium channel, voltage-dependent, T type, alpha 1H subunit |
| *Kcna5* | NM_145983 | Potassium voltage-gated channel, shaker-related subfamily, member 5 |
| *Kcne1* | NM_008424 | Potassium voltage-gated channel, Isk-related subfamily, member 1 |
| *Kcne2* | NM_134110 | Potassium voltage-gated channel, Isk-related subfamily, gene 2 |
| *Kcnd2* | NM_019697 | Potassium voltage-gated channel, Shal-related family, member 2 |
| *Kcnd3* | NM_019931 | Potassium voltage-gated channel, Shal-related family, member 3 |
| *Kcnh2* | NM_013569 | Potassium voltage-gated channel, subfamily H (eag-related), member 2 |
| *Kcnj2* | NM_008425 | Potassium inwardly-rectifying channel, subfamily J, member 2 |
| *Kcnj3* | NM_008426 | Potassium inwardly-rectifying channel, subfamily J, member 3 |
| *Kcnj11* | NM_010602 | Potassium inwardly rectifying channel, subfamily J, member 11 |
| *Kcnj12* | NM_010603 | Potassium inwardly-rectifying channel, subfamily J, member 12 |
| *Kcnj14* | NM_145963 | Potassium inwardly-rectifying channel, subfamily J, member 14 |
| *Kcnq1* | NM_008434 | Potassium voltage-gated channel, subfamily Q, member 1 |
| *Scn5a* | NM_021544 | Sodium channel, voltage-gated, type V, alpha |
| *Slc2a1* | NM_011400 | Solute carrier family 2 (facilitated glucose transporter), member 1 |
| *Slc2a2* | NM_031197 | Solute carrier family 2 (facilitated glucose transporter), member 2 |
| *Slc8a1* | NM_011406 | Solute carrier family 8 (sodium/calcium exchanger), member 1 |
| *Hcn1* | NM_010408 | Hyperpolarization-activated, cyclic nucleotide-gated K+ 1 |
| *Hcn3* | NM_008227 | Hyperpolarization-activated, cyclic nucleotide-gated K+ 3 |

| | | |
|---|---|---|
| *Hcn4* | NM_001081192 | Hyperpolarization-activated, cyclic nucleotide-gated K+ 4 |
| *Gja1* | NM_010288 | Gap junction protein, alpha 1 |
| *Gja5* | NM_008121 | Gap junction protein, alpha 5 |
| *Atp1a2* | NM_178405 | ATPase, Na+/K+ transporting, alpha 2 polypeptide |
| *Atp1a3* | NM_144921 | ATPase, Na+/K+ transporting, alpha 3 polypeptide |
| *Atp2a1* | NM_007504 | ATPase, Ca++ transporting, cardiac muscle, fast twitch 1 |
| *Atp2a2* | NM_009722 | ATPase, Ca++ transporting, cardiac muscle, slow twitch 2 |
| *Ryr2* | NM_023868 | Ryanodine receptor 2, cardiac |
| *Ckm* | NM_007710 | Creatine kinase, muscle |
| *Acsl5* | NM_027976 | Acyl-CoA synthetase long-chain family member 5 |
| *Ptk2* | NM_007982 | PTK2 protein tyrosine kinase 2 |
| *Ilk* | NM_010562 | Integrin linked kinase |
| *Ctgf* | NM_010217 | Connective tissue growth factor |
| *Itga1* | NM_001033228 | Integrin alpha 1 |
| *Itga2* | NM_008396 | Integrin alpha 2 |
| *Itga4* | NM_010576 | Integrin alpha 4 |
| *Itga5* | NM_010577 | Integrin alpha 5 (fibronectin receptor alpha) |
| *Itgav* | NM_008402 | Integrin alpha V |
| *Itgb1* | NM_010578 | Integrin beta 1 (fibronectin receptor beta) |
| *Itgb3* | NM_016780 | Integrin beta 3 |
| *Abra* | NM_175456 | Actin-binding Rho activating protein |
| *Rhoa* | NM_016802 | Ras homolog gene family, member A |
| *Cdc42* | NM_009861 | Cell division cycle 42 homolog (S. cerevisiae) |
| *Rac1* | NM_009007 | RAS-related C3 botulinum substrate 1 |
| *Rock1* | NM_009071 | Rho-associated coiled-coil containing protein kinase 1 |
| *Rock2* | NM_009072 | Rho-associated coiled-coil containing protein kinase 2 |
| *Rnd1* | NM_172612 | Rho family GTPase 1 |
| *Vcl* | NM_009502 | Vinculin |
| *Ctnnb1* | NM_007614 | Catenin (cadherin associated protein), beta 1 |
| *Aifm1* | NM_012019 | Apoptosis-inducing factor, mitochondrion-associated 1 |
| *Atp5j* | NM_016755 | ATP synthase, H+ transporting, mitochondrial F0 complex, subunit F |
| *Hsp90ab1* | NM_008302 | Heat shock protein 90 alpha (cytosolic), class B member 1 |
| *Hspa2* | NM_008301 | Heat shock protein 2 |
| *Hsph1* | NM_013559 | Heat shock 105kDa/110kDa protein 1 |
| *Bcat1* | NM_007532 | Branched chain aminotransferase 1, cytosolic |
| *Ch25h* | NM_009890 | Cholesterol 25-hydroxylase |
| *Itpr2* | NM_019923 | Inositol 1,4,5-triphosphate receptor 2 |
| *Tgfb2* | NM_009367 | Transforming growth factor, beta 2 |
| *Notch1* | NM_008714 | Notch gene homolog 1 (Drosophila) |
| *Pou5f1* | NM_013633 | POU domain, class 5, transcription factor 1 |
| *Nanog* | NM_028016 | Nanog homeobox |
| *Sox2* | NM_011443 | SRY-box containing gene 2 |
| *Gapdh* | NM_008084 | Glyceraldehyde-3-phosphate dehydrogenase |
| *Actb* | NM_007393 | Actin, beta |

**Table S2. List of major experimental measurement categories, related to Figure 5**

| Measurement Class | Measurement | Measurement Description |
|---|---|---|
| Contractility | Diastolic | Diastolic stress |
| Contractility | Systolic | Systolic stress |
| Contractility | Twitch | Twitch Stress (Systolic - Diastolic) |
| Electrophysiology | LCV | Longitudinal conduction velocity |
| Electrophysiology | TCV | Transverse conduction velocity |
| Electrophysiology | AR | Anisotropy ratio |
| Electrophysiology | APD50 | Action potential duration at 50% repolarization |
| Electrophysiology | APD90 | Action potential duration at 90% repolarization |
| Electrophysiology | TOT | Total calcium current density |
| Electrophysiology | LCC | L-type calcium current density |
| Electrophysiology | TCC | T-type calcium current density |
| Morphology | SPD | Sarcomere packing density |
| Morphology | SL | Sarcomere length |
| Morphology | OOP | Orientational order parameter |
| Gene expression | *Hey2* | Hairy/enhancer-of-split related with YRPW motif 2 |
| Gene expression | *Irx4* | Iroquois related homeobox 4 (Drosophila) |
| Gene expression | *Gata4* | GATA binding protein 4 |
| Gene expression | *Myocd* | Myocardin |
| Gene expression | *Nkx2-5* | NK2 transcription factor related, locus 5 (Drosophila) |
| Gene expression | *Tbx5* | T-box 5 |
| Gene expression | *Nppa* | Natriuretic peptide type A |
| Gene expression | *Acta1* | Actin, alpha 1, skeletal muscle |
| Gene expression | *Adra1b* | Adrenergic receptor, alpha 1b |
| Gene expression | *Adra2a* | Adrenergic receptor, alpha 2a |
| Gene expression | *Actc1* | Actin, alpha, cardiac muscle 1 |
| Gene expression | *Actn1* | Actinin, alpha 1 |
| Gene expression | *Actn2* | Actinin alpha 2 |
| Gene expression | *Pln* | Phospholamban |
| Gene expression | *Tnnt2* | Troponin T2, cardiac |
| Gene expression | *Ttn* | Titin |
| Gene expression | *Myh6* | Myosin, heavy polypeptide 6, cardiac muscle, alpha |
| Gene expression | *Myh7* | Myosin, heavy polypeptide 7, cardiac muscle, beta |
| Gene expression | *Myl2* | Myosin, light polypeptide 2, regulatory, cardiac, slow |
| Gene expression | *Myl3* | Myosin, light polypeptide 3 |
| Gene expression | *Myl4* | Myosin, light polypeptide 4 |
| Gene expression | *Myl7* | Myosin, light polypeptide 7, regulatory |
| Gene expression | *Cacna1c* | Calcium channel, voltage-dependent, L type, alpha 1C subunit |
| Gene expression | *Cacna1d* | Calcium channel, voltage-dependent, L type, alpha 1D subunit |
| Gene expression | *Cacna1g* | Calcium channel, voltage-dependent, T type, alpha 1G subunit |
| Gene expression | *Cacna1h* | Calcium channel, voltage-dependent, T type, alpha 1H subunit |

| | | |
|---|---|---|
| Gene expression | *Kcne1* | Potassium voltage-gated channel, Isk-related subfamily, member 1 |
| Gene expression | *Kcne2* | Potassium voltage-gated channel, Isk-related subfamily, gene 2 |
| Gene expression | *Kcnd2* | Potassium voltage-gated channel, Shal-related family, member 2 |
| Gene expression | *Kcnd3* | Potassium voltage-gated channel, Shal-related family, member 3 |
| Gene expression | *Kcnh2* | Potassium voltage-gated channel, subfamily H (eag-related), member 2 |
| Gene expression | *Kcnj2* | Potassium inwardly-rectifying channel, subfamily J, member 2 |
| Gene expression | *Kcnj3* | Potassium inwardly-rectifying channel, subfamily J, member 3 |
| Gene expression | *Kcnj11* | Potassium inwardly rectifying channel, subfamily J, member 11 |
| Gene expression | *Kcnj12* | Potassium inwardly-rectifying channel, subfamily J, member 12 |
| Gene expression | *Kcnj14* | Potassium inwardly-rectifying channel, subfamily J, member 14 |
| Gene expression | *Kcnq1* | Potassium voltage-gated channel, subfamily Q, member 1 |
| Gene expression | *Scn5a* | Sodium channel, voltage-gated, type V, alpha |
| Gene expression | *Slc2a1* | Solute carrier family 2 (facilitated glucose transporter), member 1 |
| Gene expression | *Slc2a2* | Solute carrier family 2 (facilitated glucose transporter), member 2 |
| Gene expression | *Slc8a1* | Solute carrier family 8 (sodium/calcium exchanger), member 1 |
| Gene expression | *Hcn1* | Hyperpolarization-activated, cyclic nucleotide-gated K+ 1 |
| Gene expression | *Hcn3* | Hyperpolarization-activated, cyclic nucleotide-gated K+ 3 |
| Gene expression | *Hcn4* | Hyperpolarization-activated, cyclic nucleotide-gated K+ 4 |
| Gene expression | *Gja1* | Gap junction protein, alpha 1 |
| Gene expression | *Gja5* | Gap junction protein, alpha 5 |
| Gene expression | *Atp1a2* | ATPase, Ca++ transporting, cardiac muscle, fast twitch 1 |
| Gene expression | *Atp2a2* | ATPase, Ca++ transporting, cardiac muscle, slow twitch 2 |
| Gene expression | *Ryr2* | Ryanodine receptor 2, cardiac |
| Gene expression | *Ckm* | Creatine kinase, muscle |

## Supplementary Movies

**Movie S1.** Anisotropic mES MTF paced at 3 Hz, related to Figure 4.
**Movie S2.** Anisotropic miPS MTF paced at 3 Hz, related to Figure 4.
**Movie S3.** Anisotropic Neonate MTF paced at 3 Hz, related to Figure 4.

## Supplementary Methods

### Calculation of isolated cell surface area, related to Figure S1

The surface area of individual Neonate, mES-, and miPS-derived cardiac myocytes was measured by seeding them at low density onto PDMS-coated coverslips treated with a uniform layer of FN, and examining fluorescence micrographs of cells immunostained for chromatin, F-actin, and sarcomeric α-actinin. Cardiac myocytes were identified by the presence of sarcomeric α-actinin positive z-lines, and the boundaries of fully spread, mono-nucleated myocytes were manually traced using the polygon tool in ImageJ. The total spread surface area for each cardiac myocyte was calculated from the total number of pixels contained within each polygon.

### Quantitative evaluation of sarcomere structure, related to Figure S2

Analysis of sarcomeric structural characteristics was conducted, after de-convolving acquired confocal Z-stacks of sarcomeric α-actinin fluorescence micrographs with Mediacy Autoquant (MediaCybernetics, Rockville, MD), on custom-designed ImageJ (Abramoff, 2004) (NIH) and MATLAB (Mathworks, Natick, MA) software (Figure S2A). Fluorescence micrographs were first pre-processed to highlight the filamentous structure of the cytoskeleton using a "tubeness" operator (Sato et al., 1998). This operator replaced each pixel in the image with the largest non-positive eigenvalue of the image Hessian matrix. The orientations of sarcomeric α-actinin positive pixels were determined using an adapted structure-tensor method (Rezakhaniha et al., 2012) and the orientational order parameter (OOP), a measure of the global alignment of the sarcomeres, was calculated from the observed orientation angles.

The orientations observed in the micrographs were color-coded using the HSV digital image representation (Figure S2Bi) where the Hue channel was used for orientation, the Saturation channel for pixel coherency (*i.e.* a measure of local contrast), and the Value channel for the pre-processed image. The normalized occurrence of the orientations that demonstrated a coherency higher than a given threshold (sub-threshold pixels were not color-coded) could then be displayed in a histogram (Figure S2Bii). Two components could be easily distinguished: blue-green coloration in (Figure S2Bi) corresponded to pixels localized to Z-disks (black curve in Figure S2Bii), while red-yellow pixels were associated with long stretches of Z-bodies (red curve in Figure S2Bii).

The sarcomere length and the overall regularity of the z-lines was determined by processing the fluorescence images with a 2D Fast Fourier Transform algorithm (the power spectrum of the image in Figure S2Bi is reported in Figure S2Ci with a gamma correction of 0.1 to improve visualization). To further analyze the Fourier representation without introducing user-bias (Wei et al., 2010), the power spectrum was then radially integrated and normalized by the total area under the 1D curve. The previous step yielded a 1D profile (blue curve in Figure S2Cii) that could be fitted with aperiodic (4, black line in Figure S2Cii) and periodic (4, red line in Figure S2Cii) components. The parameters $\{a, b, c\}$ in (4) characterize the decaying exponential chosen to model the effect of noise and non-regularly distributed structures in the image, while the parameters $\{\omega_0, a_k, \delta_k\}$ in (5) represent respectively, the wavenumber that corresponds to the sarcomere length, the amplitude and the width of the Gaussian peaks chosen

to model the periodic peaks. The sarcomere packing density was defined as the area under the periodic component (shaded red in Figure S2Cii).

$$\tilde{\Gamma}_{ap}\left(\omega,\gamma_{ap}\right)=a+be^{-c\omega};\qquad \gamma_{ap}=\{a,b,c\} \tag{4}$$

$$\tilde{\Gamma}_{p}\left(\omega,\gamma_{p}\right)=\sum_{k=1}^{3}a_k e^{-\left(\frac{\omega-k\omega_0}{\delta_k}\right)^2};\qquad \gamma_{ap}=\{\omega_0,a_k,\delta_k\} \tag{5}$$

**Statistical analysis**

All data are summarized as mean ±standard error of the mean. Data were first tested for normality (Shapiro-Wilk) and equal variance (Levene Median test). Based on the results from these tests, either 1-way ANOVA or ANOVA on Ranks were adopted to establish statistical difference between the groups. Pairwise comparisons were then assessed using either Dunn's or Tukey or Holm-Sidak methods as post-hoc tests. In the figures the significance of statistical tests (p-value) is indicated as follows: * = $p < 0.05$, ** = $p < 0.001$ for 1-way ANOVA and for † = $p < 0.05$, †† = $p < 0.001$ ANOVA on ranks.

**Supplemental References**

Abramoff, M.D., Magalhaes, P.J., Ram, S.J. (2004). Image Processing with ImageJ. Biophotonics International *11*, 36-42.

Rezakhaniha, R., Agianniotis, A., Schrauwen, J.T.C., Griffa, A., Sage, D., Bouten, C.V.C., van de Vosse, F.N., Unser, M., and Stergiopulos, N. (2012). Experimental investigation of collagen waviness and orientation in the arterial adventitia using confocal laser scanning microscopy. Biomech Model Mechanobiol *11*, 461-473.

Sato, Y., Nakajima, S., Shiraga, N., Atsumi, H., Yoshida, S., Koller, T., Gerig, G., and Kikinis, R. (1998). Three-dimensional multi-scale line filter for segmentation and visualization of curvilinear structures in medical images. Medical image analysis *2*, 143-168.

Wei, S., Guo, A., Chen, B., Kutschke, W., Xie, Y.P., Zimmerman, K., Weiss, R.M., Anderson, M.E., Cheng, H., and Song, L.S. (2010). T-tubule remodeling during transition from hypertrophy to heart failure. Circ Res *107*, 520-531.